



Integrated polysaccharides via amidation for sensitive electrochemical detection of heavy metal ions

Jinliang Chen¹, Mengmeng Zhang¹, Quanxing Liao¹, Letong Wang¹, Hongxia Li¹, Xiaohui Niu¹, Xiaoyu Liu¹, and Kunjie Wang^{1,*}

¹ College of Petrochemical Technology, Lanzhou University of Technology, 730050 Lanzhou, People's Republic of China

Received: 22 December 2021

Accepted: 19 February 2022

Published online:

1 March 2022

© The Author(s), under exclusive licence to Springer Science+Business Media, LLC, part of Springer Nature 2022

ABSTRACT

In this work, polysaccharide sodium alginate(SA) and chitosan(CS) were amidated and crosslinked to form honeycomb structure with hollow structure sodium alginate-chitosan complex (SA-CS). The honeycomb structure with hollow structure generated by crosslinked polysaccharides exposed the polar functional groups of SA and CS compared with individual SA and CS, resulting in a significant increase in the hydrophilicity of SA-CS. Excessive intake and accumulation of Cu^{2+} will cause health hazards to the human body, animals and plants, and some diseases will appear. Therefore, we need to develop suitable detection methods. We modified the integrated polysaccharide complex SA-CS on the surface of the glassy carbon electrode (GCE), and optimized the experimental conditions of SA-CS/GCE for the detection of heavy metal copper ions by differential pulse voltammetry (DPV). Since the cross-linked SA-CS increases the recognition sites for Cu^{2+} while exposing functional groups, it has high selective coordination ability for SA-CS/GCE to Cu^{2+} , and can realize the selective detection of Cu^{2+} . There is a good linear relationship between a series of different concentrations of Cu^{2+} and peak current, the linear range is $1\text{--}100\ \mu\text{mol L}^{-1}$, the obtained standard curve is $i_{\text{pc}}(\mu\text{A}) = 0.08172X (\mu\text{mol L}^{-1}) + 2.201$, $R^2 = 0.9919$, the detection limit is $0.9545\ \mu\text{mol L}^{-1}$ when the signal-to-noise ratio is at 3. Therefore, the SA-CS polysaccharide complex is expected to be constructed as a non-toxic, non-polluting, electrochemical sensor that selectively detects heavy metal copper ions in water.

1 Introduction

Natural polysaccharide is one of the most abundant natural macromolecules in the world, such as starch, cellulose, chitosan, etc. [1]. It has excellent properties such as microbial degradability, biofunctionality, and

environmental and biocompatibility [2, 3]. It can be widely used to various fields closely related to human life, such as sewage treatment [4], biology [5], environment, medicine [6], food industry [7], chemistry and chemical industry. However, the individual polysaccharide will produce agglomeration effect

Address correspondence to E-mail: wangkj80@163.com

due to the intermolecular forces, which will limit its recognition application [8]. Therefore, the use of covalent bonds to compound polysaccharides can not only increase the recognition site of the sensing interface, but also solve the agglomeration effect and improve its function.

The heavy metal copper ion has gradually become one of the main pollutants in the water environment. Like other heavy metals, copper is also toxic and non-degradable. It can be enriched through the food chain even in a low-concentration environment, so it will cause great harm to the human body [9]. When a large amount of heavy metal copper remains in the human body, it is easy to cause various diseases, such as chronic diseases (diabetes, cardiovascular disease and arteriosclerosis, etc.) [10], neurological disorders (such as Alzheimer's disease) [11], and even cancer [12]. According to the previous reports [13], when the body's copper content exceeds 100 to 150 times than the required amount, it can cause necrotizing hepatitis and hemolytic anemia. Therefore, it is necessary to detect the Cu content in water quickly, accurately, conveniently and cost-effectively.

There are also various methods that can realize the detection of heavy metal copper ions. Including spectroscopy [14], atomic spectroscopy [15], fluorescence spectroscopy [16], inductively coupled plasma mass spectrometry [17], chromatography [18] and electrochemical analysis methods [19]. In recent years, some new detection methods have also appeared, such as biosensor method [20], immunoassay method [21], enzyme inhibition method [22] and so on. However, the electrochemical analysis method has the advantages of high sensitivity, fast analysis speed, good resolution, simple operation, low instrument price, and the measurement signal does not need to be analyzed and converted, which can directly record and measure multiple elements in the field of analysis. According to the different electrochemical signals detected, electrochemical amperometry analysis methods are generally divided into voltammetry, amperometric analysis, resistance analysis, potential analysis, conductance analysis, etc. [23]. Among them, the main application in the detection of heavy metals is anode stripping voltammetry and ion selective electrode [24]. Because differential pulse voltammetry can eliminate the interference of high salt content in the detection environment, it can measure both free state metal ions and complex metals, and is often used for

qualitative analysis of trace metals [25]. Therefore, this work adopts differential pulse voltammetry to identify copper ions.

In recent years, the combination of polysaccharides has been applied in many fields, which has attracted the attention of researchers. For example, chitosan and sodium alginate are compounded to prepare aerogels, which are used as antibacterial materials and loaded drugs [26]. SA-CMC gel beads are prepared by blending and cross-linking sodium alginate (SA) and sodium carboxymethyl cellulose (CMC), and the prepared SA-CMC gel beads have successfully achieved effective removal of Pb^{2+} [27]. However, there are not many studies on using polysaccharide complexes for heavy metal ions.

In this work, we connected sodium alginate and chitosan through the amidation reaction of the carboxyl and amino groups on them to prepare the polysaccharide complex sodium alginate-chitosan (SA-CS). The as-prepared SA-CS presents a honeycomb structure with hollow structure. While increasing the hydrophilicity, it provides more recognition sites for the recognition of heavy metal ions, which is more conducive to the detection of metal ions [28]. We successfully verified the recognition of Cu^{2+} by differential pulse voltammetry and the polysaccharide complex SA-CS was constructed as an electrochemical sensor for electrode materials [28].

2 Experimental section

2.1 Reagents and apparatus

Sodium alginate (SA) and chitosan (CS) were obtained from Aladdin Chemical Co., Ltd. (Shanghai, China), N-hydroxysuccinimide (NHS, 98%), 1-ethyl-3-(3-(dimethylamino) propyl) carbodiimide (EDC, 98%), Sodium acetate, glacial acetic acid and $CuCl_2$ were obtained from Sinopharm Chemical Reagent Co., Ltd. (Shanghai, China). Other chemicals not mentioned are of analytical grade and do not require further purification. All solutions were prepared using deionized water (18.2m Ω), and all experiments were performed at room temperature (20 °C).

A SCIENTZ-12 N freeze-drying machine was used to freeze-dry the polysaccharides. The traditional three-electrode system were used in electrochemical experiments, including platinum wire as counter

electrode, saturated calomel electrode as reference electrode and SA-CS modified glassy carbon electrode(SA-CS/GCE) as the working electrode. The cyclic voltammetry and differential pulse voltammetry are performed on CHI 660E electrochemical workstation. We used an X-ray diffractometer (D8 ADVANCE) to record XRD patterns in the range of 5.0 to 80.0° at a scan rate of 10°/min. Fourier transform infrared spectroscopy (FT-IR) (FTIR-650S) were used to identify the surface groups of the freeze-dried SA-CS polysaccharide complex at a wavelength of 4000–500 cm⁻¹. Scanning electron microscope (SEM) (ZEISS Sigam 300) was used to study the three-dimensional network structure and morphology of SA-CS polysaccharide complex, and PHS-25 acidity meter was used to prepare different pH carboxylic acid buffer solution.

2.2 Preparation of polysaccharide complex of sodium alginate and chitosan (SA-CS) by amidation method

100 mg SA was completely dissolved in 40 mL deionized water at 40 °C, and then 50mgNHS and EDC were slowly added at room temperature. The -COOH on SA was completely activated by constant temperature stirring for 4 h. Next, different amounts of CS (50 mg, 100 mg, 150 mg, 200 mg) were dissolved in 50 ml of 0.1 M acetic acid solution and stirred for 4 h. Then, the prepared CS solution was slowly added drop by drop into the activated SA solution, and stirred vigorously at room temperature for 4 h. The -NH₂ of chitosan(CS) and the -COOH of sodium alginate(SA) will complete amidation reaction and cross link to form SA-CS. The centrifuged product is then washed with deionized water and acetic acid. Lastly, the prepared SA-CS polysaccharide complex was freeze-dried and labeled as SA-CS (1:0.5), SA-CS (1:1), SA-CS (1:1.5), SA-CS (1: 2) [28, 29].

2.3 10⁻³ mmol/L potassium ferricyanide and potassium ferrocyanide solution

0.8231 g potassium ferricyanide and 1.0560 g potassium ferrocyanide solid and 1.9 g KCl were accurately weighed, which were dissolved in deionized water and transfer to 250 mL volumetric flask.

2.4 1.3 Electrochemical recognition of Cu²⁺ by polysaccharide complex SA-CS

The polysaccharide complex SA-CS (10 mg) was dispersed in 5 mL of deionized water, and then we use a pipette to take 10 μL of this dispersion and apply it directly on the surface of the bare glassy carbon electrode with a diameter of 3 mm. Before being modified, the suede was polished into a mirror with 0.3 μm and 0.05 μm Al₂O₃ powder, respectively. After washing the surface dirt, it was transferred to an ultrasonic water bath and washed with ultrapure water for 2 min. Finally, the modified electrode was placed at room temperature for 5 min to completely evaporate the solvent on the electrode surface to obtain a composite material modified electrode, which is the working electrode.

By immersing the electrode in an electrolyte containing a predetermined concentration of Cu²⁺, differential pulse stripping voltammetry was used to identify Cu²⁺. The parameters of differential pulse stripping voltammetry: deposition potential: -0.8 V, initial potential: -0.4 V, termination potential: 0.4 V, potential increment: 4 mV, deposition time: 300 s, pulse period: 0.5 s, waiting time: 20 s, cleaning potential: 1.0 V, cleaning time: 120 s, amplitude: 50 mV, frequency: 15 Hz.

3 Results and discussion

3.1 Structural analysis of SA-CS polysaccharide complex

Under the hydrogen bond force between the macromolecular chains of SA and CS, the two polysaccharide substances easily form agglomerations, which can be seen from SEM images (Fig. 1a and b). However, it presents honeycomb structure with hollow structure composed of micron-sized interwoven fibers (Fig. 1c), when SA and CS are compounded to SA-CS. It shows that covalent cross-linking effectively reduces the agglomeration of polysaccharides, and the cross-linked network structure is beneficial to increase recognition sites and better recognize Cu²⁺.

In the process of forming the integrated polysaccharide of SA-CS through the amidation of the carboxyl group on the sodium alginate and the amino group on the chitosan, the gap between the macromolecular chains of sodium alginate (or chitosan)

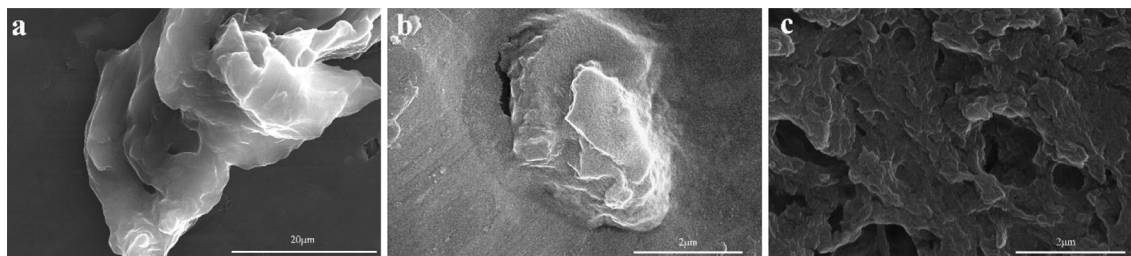


Fig. 1 Scanning electron micrographs of SA (a), CS (b), SA-CS (c)

Intrinsic intermolecular hydrogen bonds are broken because of newly formed amide bond, resulting in the expansion of the internal space between the SA-CS macromolecular chains, forming the honeycomb structure with hollow structure of SA-CS, as shown in Fig. 2 [30].

3.2 Enhanced hydrophilicity of polysaccharide complex SA-CS

Through the contact angle test of CS, SA and SA-CS, the change of its hydrophilicity was evaluated. According to Fig. 3, it can be seen that compared with the contact angles of SA and CS, the contact angle of SA-CS is significantly reduced to 55.4°, and the hydrophilicity of the surface SA-CS is significantly enhanced. However, the contact angle of SA-CS is not between SA and CS, but is smaller than the

contact angle of the two. This result also shows that it is not a simple mixture of the two but the product of its amidation, also indirectly proved the successful synthesis of polysaccharide complexes. Because SA and CS generate a honeycomb structure with hollow structure polysaccharide complex through amidation reaction, more polar functional groups (-COOH, -OH, -NH₂, etc.) are exposed to the surface of SA-CS, making SA-CS hydrophilic. The performance is greatly increased, which also provides reliability for the detection of Cu²⁺ in practical applications.

3.3 Structural characterization of polysaccharide complex SA-CS

FT-IR characterizes the functional groups of SA, CS and SA-CS, as shown in Fig. 4a. In the CS spectrum, the characteristic peaks of -OH/-NH₂, -CH₂ and C=O

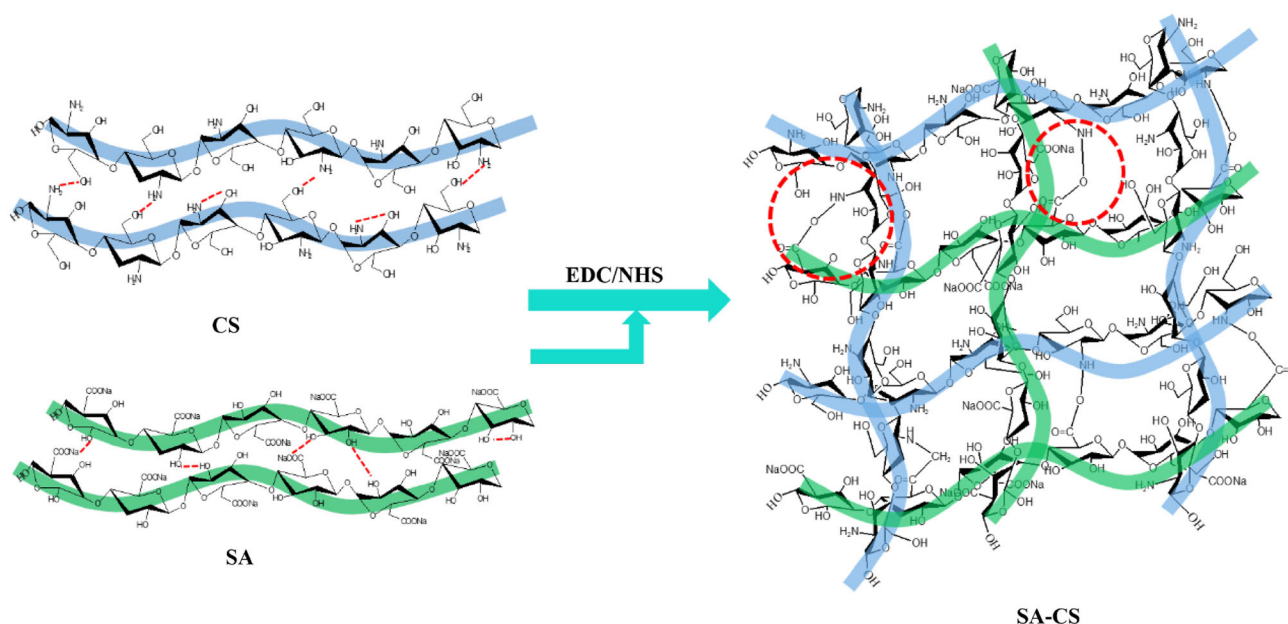


Fig. 2 Formation of honeycomb structure with hollow structure of SA-CS accompanied by the breaking of intrinsic intermolecular H bonds between the macromolecular chains of CS and SA

Fig. 3 Contact angle images of CS (a), SA (b), SA-CS (c)

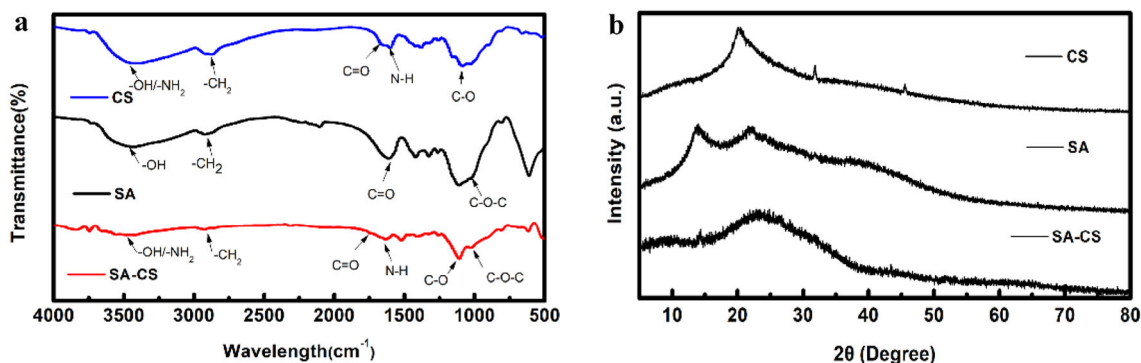
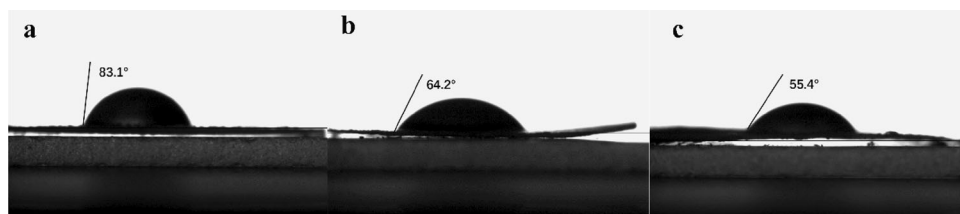


Fig. 4 a FT-IR spectra of CS, SA and SA-CS. b XRD spectra of CS, SA and SA-CS

appeared at 3429.9 cm^{-1} , 2875.1 cm^{-1} and 1029 cm^{-1} . And the characteristic peaks appearing at 1650 cm^{-1} and 1602 cm^{-1} are attributed to the C=O stretching vibration peak of -CONH- and the N-H bending vibration peak of -NH₂. For SA, the characteristic peaks of -OH, -CH₂ and C-O-C appeared at 3423.2 cm^{-1} , 2923.8 cm^{-1} and 1060 cm^{-1} . The antisymmetric and symmetric stretching vibration peaks of -COO⁻ appear at 1620 and 1430 cm^{-1} . SA-CS has characteristic peaks similar to CS. However, the flexural vibration peak of N-H is blue shifted from 1602 cm^{-1} to 1611 cm^{-1} , and overlaps with the C=O stretching vibration peak on -CONH-. The blue shift of N-H bending vibration on SA-CS indicates the successful synthesis of SA-CS [31]. According to the XRD patterns of CS, SA, and SA-CS (Fig. 4b), the three substances all have typical diffraction peaks at 23° , and the diffraction peaks of CS and SA also exist in SA-CS, which further proves the successful preparation of SA-CS [32].

In order to further study the successful combination of SA and CS, the C1s, O1s and N1s spectra of SA-CS were characterized by XPS spectra. It can be seen from Fig. 5a that SA-CS has three characteristic peaks at 284.0 eV , 530.0 eV , and 399.0 eV , which are the characteristic peaks of C1s, O1s and N1s. It can be seen from Fig. 5b, the high-resolution C 1 s spectrum has four different forms of carbon components at 284.4 eV , 282.6 eV , 285.8 eV , and 284.1 eV ,

corresponding to C-N, C=O, C-O and C-C respectively. The regional XPS spectrum of N1s is shown in Fig. 5d. It can be seen that high-resolution N1s has two forms of nitrogen at 399.4 eV and 397.2 eV , corresponding to C-N and -NH₂, respectively [33]. As shown in Fig. 5c that the O1s spectrum of SA-CS can be divided into three peaks at different positions, which indicates that the O atom exists in three different valence states, namely N-C=O (528.4 eV), C-O-C (528.9 eV), -C-OH (530.5 eV), further proved the successful synthesis of SA-CS [28].

3.4 Analysis of electrochemical performance of different modified electrodes

To investigate the electrochemical performance of chitosan modified glassy carbon electrode (CS/GCE), sodium alginate modified glassy carbon electrode (SA/GCE) and SA-CS composite modified glassy carbon electrode (SA-CS/GCE), we put these three working electrodes in the solution containing $\text{Fe}(\text{CN})_6^{3-/4-}$, and perform cyclic voltammetry test when the potential window range is -0.2 – 0.6 V and the scan rate is 50 mV s^{-1} . It can be seen from Fig. 6a, since the -COOH, -OH, -OR and other functional groups on the SA surface can hinder electron transfer, the redox peak of SA-modified electrode is smaller than that of CS-modified electrode. When CS and SA

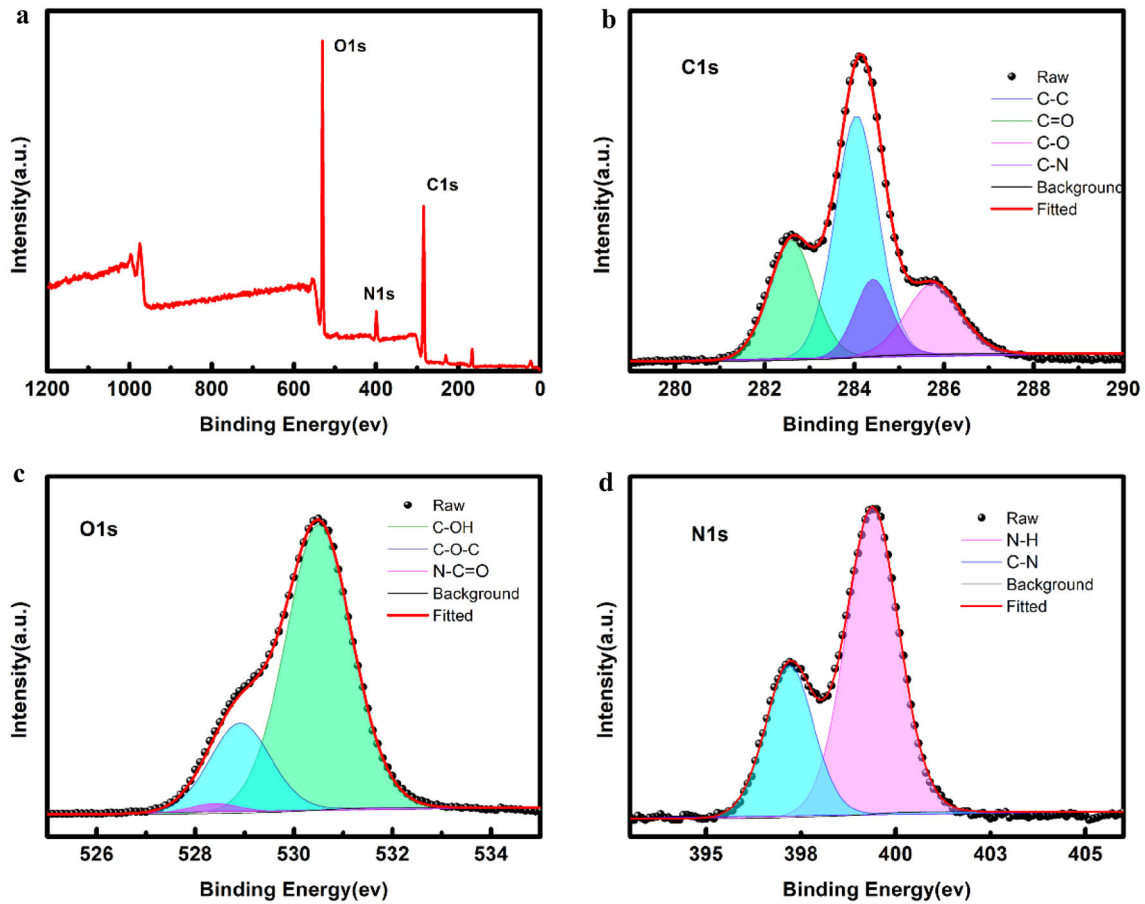


Fig. 5 a XPS survey spectrum; b High-resolution C1s peaks and fitting curves; c High-resolution O1s peaks and fitting curves; d High-resolution N1s peaks and fitting curves

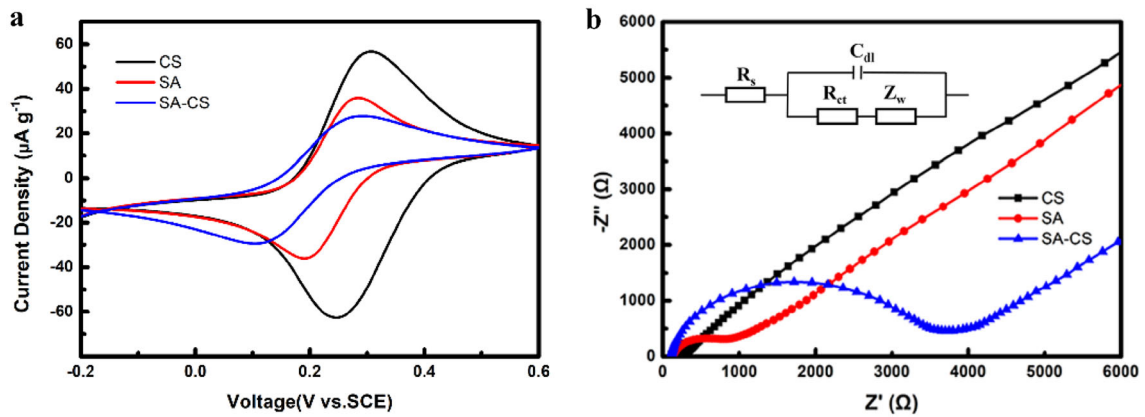


Fig. 6 a The cyclic voltammety curve of CS, SA, SA-CS modified bare glassy carbon electrode in 10 mmol L⁻¹ Fe(CN)₆^{3-/4-} solution containing 0.1 mol/L KCl; b EIS spectra of CS, SA,

SA-CS modified bare glassy carbon electrode in 10 mmol/L Fe(CN)₆^{3-/4-} solution containing 0.1 mol/L KCl

are combined, honeycomb structure with hollow structure of cross-linked structure further hinders the transfer of electrons, so the redox peak of SA-CS is the smallest.

In order to further study the electrochemical properties of different materials and their value as electrode materials, we conducted cyclic voltammetry test and electrochemical impedance test for

them. Electrochemical impedance spectroscopy (EIS) is used to judge the conductivity of materials in the process of redox. The Nyquist diagram of Fig. 6b consists of the low-frequency region of an approximate straight line and the high-frequency region of a semicircle. R_s is the equivalent resistance of the series model, representing the intersection of the extension line and X-axis in the low-frequency region, that is the inherent resistance of the electrode material, the electrolytic cell resistance and the electrode/electrolyte interface contact resistance. R_{ct} is the charge transfer resistance, represented by the diameter of the high frequency region. Z_w stands for the diffusion of ions. The higher the slope of the line in the low-frequency region, the higher the diffusion rate of ions in the electrolyte. C_{dl} was the double layer capacitance. Due to honeycomb structure with hollow structure of cross-linked structure further hinders the transfer of electrons, so the order of the R_{ct} was as displayed in the following: SA-CS/GCE > SA/GCE > CS/GCE. This has also been further demonstrated by the CV result of SA, CS and SA-CS (Fig. 6a).

3.5 Optimization of experimental conditions

In order to improve the detection sensitivity, we optimized some experimental parameter that affect the electrochemical signal of copper ions, such as the pH of the electrolyte solution used when detecting copper ions, the deposition potential and deposition time on the SA-CS modified electrode [34].

Figure 7a is the optimized curve of SA-CS modified electrode(SA-CS/GCE) in 0.1 mol L⁻¹ acetate buffer solution of different pH containing 50 μmol L⁻¹ copper ion. It can be seen from the figure that the pH of the buffer solution has a great influence on the

reduction of Cu²⁺ adsorbed on the electrode surface. During the gradual increase of pH, the dissolution peak current of Cu²⁺ first increased and then decreased, and the peak current reached the maximum at pH 5.0. This may be because in the pH = 5.0 buffer solution, the metal copper deposited on the electrode surface is completely converted into copper ions. The most important is that the branched SA-CS has the strongest complexing ability to heavy metal Cu²⁺ in this pH environment. Therefore, the peak dissolution current is the largest at this time. In a strongly acidic environment with a pH of less than 5.0, there will be a competitive reaction between hydrogen ions and copper ions in the solution. Therefore, the amount of copper ions deposited on the surface of a limited SA-CS modified electrode will be relatively reduced, thereby the stronger the acidity, the material will decompose and the stability will not be high, affecting the dissolution of copper. In a solution with a pH greater than 5.0, a small part of the dissolved Cu²⁺ will be hydrolyzed, which will reduce the peak current of the dissolution. Therefore, we choose an acetate buffer solution with a pH of 5.0 as the electrolyte.

Figure 7b is the optimized curve of the SA-CS modified electrode(SA-CS/GCE) at pH = 5.0 and the deposition potential changes from -0.3 to -1.0 V. It can be seen that with the negative shift of the deposition potential, the dissolution peak current of Cu²⁺ gradually increases, and the peak current reaches the maximum when the deposition potential is -0.8 V. Even if the deposition potential is more negative than -1.0 V, the peak current tends to increase. But at a more negative potential, the hydrogen evolution competition reaction on the surface of the SA-CS modified electrode will reduce the peak current value, thereby affecting the copper ion

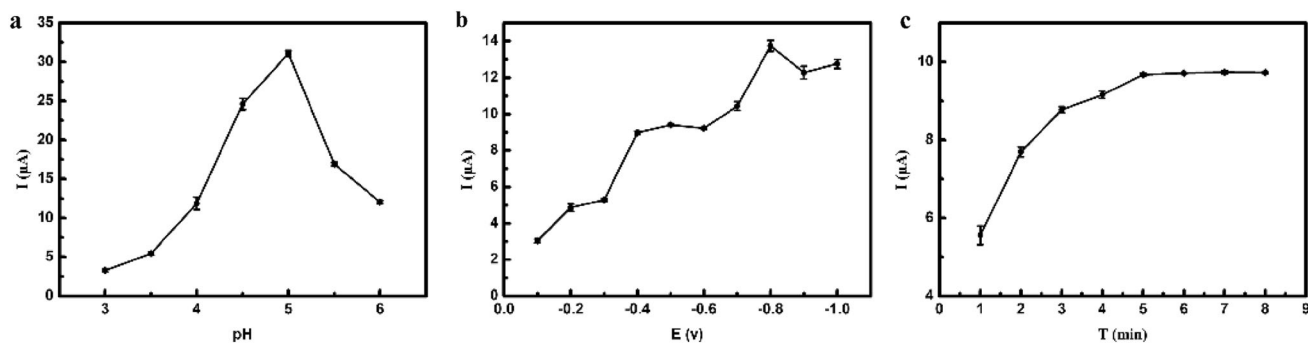


Fig. 7 The influence of buffer pH **a**, deposition potential **b** and deposition time **c** on the detection of copper ions by SA-CS/GCE

detection signal, so we think -0.8 V is the optimal deposition potential.

Figure 7c is the optimized curve of the deposition time of $50 \mu\text{mol L}^{-1} \text{Cu}^{2+}$ in the process of increasing the deposition time from 1 to 8 min when the SA-CS modified electrode is at $\text{pH} = 5.0$ and the deposition potential is -0.8 V. As show in Fig. 7c that the peak current increases as the deposition time increases from 1 to 8 min. Because with the extension of the deposition time, more and more Cu^{2+} is enriched on the modified electrode, and the more Cu^{2+} during the dissolution process can be obtained, and the greater the peak dissolution current can be observed. The peak current value reached the maximum when the deposition time was increased to 5 min, and Cu^{2+} reached saturation on the surface of the modified electrode. Taking into account the stability, timeliness and sensitivity of the modified electrode, we choose the best deposition time of 5 min. Because the curve of dissolution current and time is linear when the deposition time is extended to 5 min.

3.6 Study on the selectivity and interference of SA-CS for Cu^{2+} detection

The $-\text{NH}_2$ of CS and $-\text{COOH}$ of SA are cross-linked to form a honeycomb structure with hollow structure through amidation reaction, exposing more functional groups and increasing recognition sites. When Cu^{2+} exists around the polysaccharide complex, Cu^{2+} can interact with the $-\text{COOH}$, $-\text{NH}_2$ and $-\text{OH}$ functional groups on the polysaccharide complex SA-CS to form surface complexes, ion exchange and electrostatic attraction (Fig. 8), the complex of SA-CS- Cu^{2+} can be formed; or form a bridge between the polysaccharide complex SA-CS ligand and the binding pocket. Therefore, Cu^{2+} can be identified though DPV by modifying SA-CS on the surface of GCE, thereby constructing an electrochemical sensor that can identify metals.

The anti-interference ability is an important indicator that determines the practicality of the sensor. The differential pulse voltammetry we chose can eliminate the interference of anions in the solution. Therefore, we have carried out selective and interference experiments on some metal cations that may affect the detection of Cu^{2+} by SA-CS /GCE.

Figure 9a shows the electrochemical response of SA-CS/GCE to Cu^{2+} in the solution when 10 times

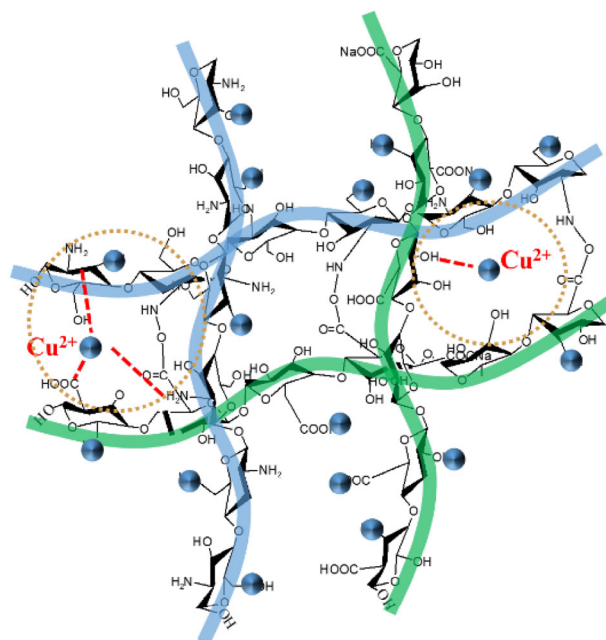


Fig. 8 SA-CS recognition mechanism diagram

other metal ions coexist in a 0.1 mol L^{-1} acetate buffer solution containing $50 \mu\text{mol L}^{-1} \text{Cu}^{2+}$. The I and I_0 are represents the peak current of Cu^{2+} dissolution in the presence and absence of other interfering ions, respectively. Studies have found that these coexisting metal ions have almost no effect on the peak current signal of Cu^{2+} .

3.7 Standard curve and detection limit

Under optimized experimental conditions, SA-CS/GCE was used to detect different concentration gradients of Cu^{2+} by differential pulse anodic stripping voltammetry, as shown in Fig. 9. It can be seen from Fig. 9b that as the concentration of Cu^{2+} gradually increases from $1 \mu\text{mol L}^{-1}$ to $100 \mu\text{mol L}^{-1}$, the peak current of the SA-CS modified electrode for Cu^{2+} detection is gradually increasing, and the peak shape of the dissolution peak is becoming more shaper. Figure 9c is a linear relationship curve between different concentrations of Cu^{2+} and the peak current. The linear regression equation obtained is $i_{\text{pc}}(-\mu\text{A}) = 0.08172X (\mu\text{mol L}^{-1}) + 2.201$, $R^2 = 0.9919$ the detection limit is $0.9545 \mu\text{mol L}^{-1}$, when the signal-to-noise ratio is 3,. This shows that the SA-CS modified glassy carbon electrode can realize the quantitative analysis of low concentration Cu^{2+} , with a wide linear range and high detection sensitivity.

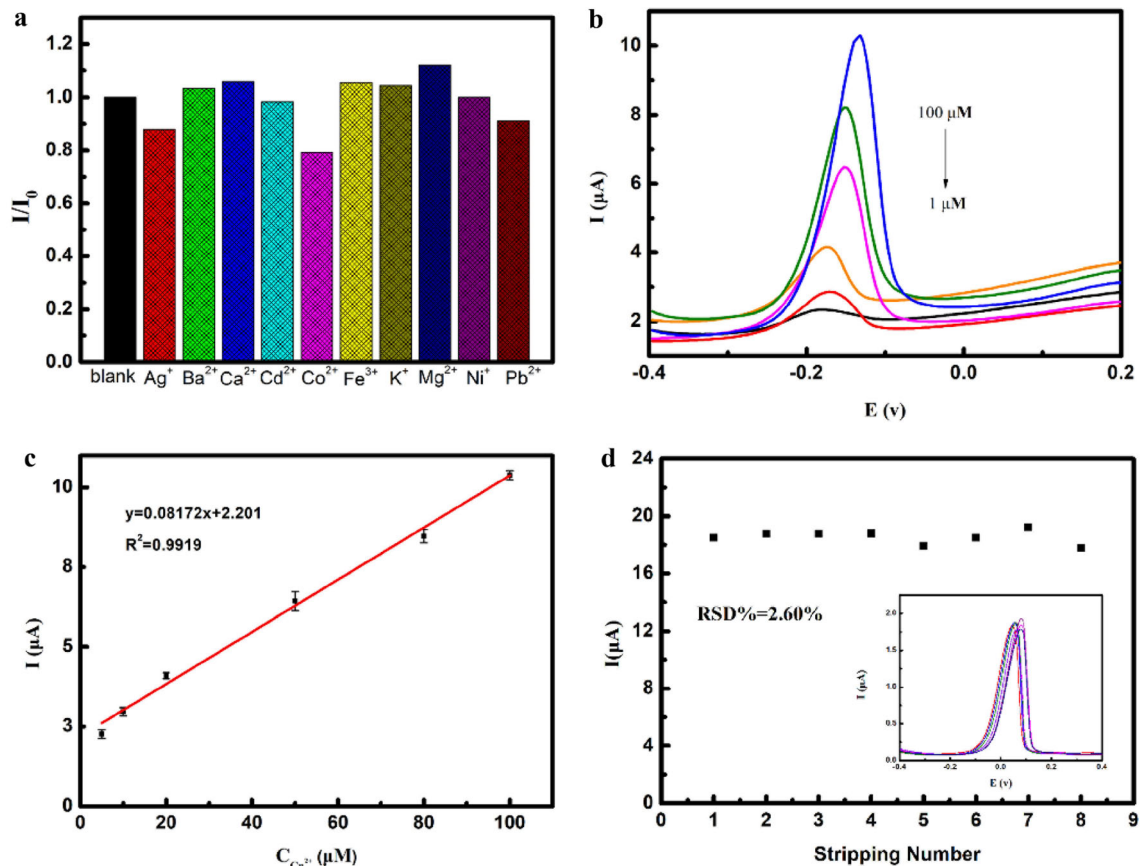


Fig. 9 **a** When adding 10 times the concentration of different metal cations, the differential pulse anodic stripping voltammetry study of Cu^{2+} by SA-CS/GCE. Among them, I and I_0 respectively represent the peak dissolution current of Cu^{2+} in the presence and absence of other interfering ions. **b** The differential pulse voltammetry curve of SA-CS/GCE to different concentrations of copper ions in 0.1 mol/L acetic acid-sodium acetate buffer solution

(PH = 5), from 100 $\mu\text{mol/L}$ to 1 $\mu\text{mol/L}$. **c** The relationship curve between copper ion concentration and corresponding peak current. **d** Under optimized experimental conditions, the stability test of SA-CS/GCE for copper ion detection. The illustration is the 8 repetitive DPV response curve of SA-CS/GCE to 50 $\mu\text{mol L}^{-1}$ Cu^{2+}

3.8 Repetitive experiment

In order to test the stability of the prepared sensor for Cu^{2+} detection, under the optimal experimental conditions, we have repeated the test for 8 times via using the same electrode (SA-CS/GCE) to test 50 $\mu\text{mol L}^{-1}$ Cu^{2+} in 0.1 mol/L NaAc-HAc buffer solution. As show in the inset of Fig. 9d that the peak current changes very little after 8 repeated detections, and the calculated relative standard deviation (RSD) is 2.60%. From Table 1, we can find that the polysaccharide complex SA-CS as an electrochemical sensor has lower detection limit and wider detection range compared with other sensors. Therefore, the SA-CS modified electrode has good repeatability and

high electrochemical stability for the DPV detection of heavy metal copper ions.

4 Conclusion

In summary, we combined the amidation of sodium alginate and chitosan to form a polysaccharide complex SA-CS, and modified it on a glassy carbon electrode to construct a new and effective electrochemical sensor for recognizing Cu^{2+} . Due to the expansion of the internal space between the macromolecular chains and the exposure of the polar functional groups during the amidation process, the polysaccharide complex forms a new honeycomb structure with hollow structure, which increases the

Table 1 Comparison of different sensor for Cu²⁺ detection

Sensor	LOD(μM)	Linear range(μM)	Application	References
THB	0.48	0–30	deionized water	[35]
PPN	0.86	0–50	deionized water	[36]
Chol-6RN	1.12	5.0–40	Live cells	[37]
CDs	0.145	6.0–33	deionized water	[38]
EG/RGO	0.98	3.0–10	deionized water	[39]
SA-CS	0.954	0–100	This Work	

recognition sites and is more conducive to the recognition of Cu²⁺. Compared with SA and CS alone, it has better hydrophilicity, so it is used as a sensing material for detecting heavy metal Cu²⁺. The polysaccharide composite material (SA-CS) has good sensitivity in the DPV detection of heavy metal Cu²⁺ with a wide detection range, low detection limit, good detection reproducibility, and a standard deviation of 2.60%, so it can be used as the electrochemical sensors to detect Cu²⁺. Since both sodium alginate and chitosan have a good biocompatibility, electrochemical sensors based on sodium alginate-chitosan integrated polysaccharide modification also opened up new ways for the detection of heavy metal ions.

Acknowledgements

This work was supported by the National Nature Science Foundations of China (Grants No. 21867015, 22065021), the Province Nature Science Foundations of Gansu (Grants No. 20JR5RA453) and Hongliu Outstanding Youth Teacher Cultivate Project of Lanzhou University of Technology.

Author contributions

All authors contributed to the study conception and design. Material preparation, data collection and analysis were performed by KW, XN and JC. The first draft of the manuscript was written by JC and all authors commented on previous versions of the manuscript. All authors read and approved the final manuscript.

Funding

The authors have not disclosed any funding.

Data Availability

All data generated or analysed during this study are included in this published article.

Declarations

Conflict of interest No conflict of interest exists in the submission of this manuscript, and manuscript is approved by all authors for publication.

Ethical approval All the authors listed have approved the manuscript that is enclosed.

References

1. V.P. Chakka, T. Zhou, *Int. J. Biol. Macromol.* **165**, 2425–2431 (2020)
2. F. Chen, G. Huang, *Int. J. Biol. Macromol.* **112**, 211–216 (2018)
3. R. Xiao, M.W. Grinstaff (2017) *Progress in Polymer Science*
4. M. Vakili, M. Rafatullah, B. Salamatinia, A.Z. Abdullah, M.H. Ibrahim, K.B. Tan, Z. Gholami, P. Amouzgar, *Carbohydr Polym* **113**, 115–130 (2014)
5. L.E. Puluhalawa, I.M. Joni, A. Mohammed, H. Arima, N. Wathoni, *Molecules* **26**, 3362 (2021)
6. S. Yu, X. Xu, J. Feng, M. Liu, K. Hu (2019) *International Journal of Pharmaceutics*
7. X. Lu, J. Chen, Z. Guo, Y. Zheng, M.C. Rea, H. Su, X. Zheng, B. Zheng, S. Miao (2019) *Trends in Food Science & Technology*
8. X. He, T. Chen, T. Jiang, C. Wang, Z. Liu, *Carbohydr. Polym.* **260**, 117790 (2021)
9. W.P.C. A, S.J.R. C, W.V.D.S.P. A, E.S.D.S. B, G.C.M. C, O.M.M.T. D, C.B.D.A. E, Y.N.D. A, A.R.F. A (2021) *J Hazardous Mater.* 126688.
10. Y. Li, Z.L. Kang, N. Qiao, L.M. Hu, Y.J. Ma, X.H. Liang, J.L. Liu, Z.M. Yang, *Biol. Trace Elem. Res.* **177**, 10–15 (2017)
11. K.J. Barnham, A.I. Bush, *Chem. Soc. Rev.* **43**, 6727–6749 (2014)
12. K. Jomova, M. Valko, *Toxicology -Shannon-* **283**, 65 (2011)

13. Y. Li, C. Yang, S. Wang, D. Yang, K. Huang (2020) *International Journal of Biological Macromolecules* 163
14. L.A. Malik, A. Bashir, A. Qureshi, A.H. Pandith, *Environ. Chem. Lett.* **17**, 1495–1521 (2019)
15. J. Hu, P. Yang, X. Hou (2019) *Applied Spectroscopy Reviews* 1–24
16. B. Hxa, L.A. Ping, T.A. Bo, *Coordination Chemistry Reviews* 427
17. P.Y. Sharanov, D.S. Volkov, N.V. Alov, *Anal. Methods* **11**, 3750 (2019)
18. T.G. Enge, M.P. Field, D. Jolley, H. Ecroyd, M.H. Kim, A. Dosseto, *J. Anal. At. Spectrom.* **31**, 2023–2030 (2016)
19. Z. Li, M. Zhu, *Chemical Communications*.
20. Z. Khoshbin, M.R. Housaindokht, M. Izadyar, M.R. Bozorgmehr, A. Verdian, *Biotechnol. Bioengin.* **118**, 555 (2021)
21. W.W. Zhao, J.J. Xu, H.Y. Chen, *Analy. Chem.* **7**, 0467 (2017)
22. Z. Junqiu, Z. Muhua, C. Xiangjian, Li. Mengyuan, Meiping. *J. Am. Chem. Soc.* **140**, 16925–16928 (2018)
23. Bansod, BabanKumar, Kumar, Tejinder, Thakur, Ritula, Rana, Shakshi, Singh, Inderbir.
24. A. Xw, B. Yq, S.B. You, Y.A. Yue, A. Lz, A. Cz, B. Ys, *Sensors and Actuators B: Chemical* 310.
25. A. Yy, Z.B. Yong, A. Zz, A. Yw, D. Gzac, (2021)
26. A. Jp, L.A. Yang, A. Kc, A. Yz, Z. Hui, *Carbohydr. Polym.* **11**, 69 (2021)
27. Z. Gao, J. Jiang, C. Luo, H. Ren, D. Wu, *Carbohydrate Polymers Scientific & Technological Aspects of Industrially Important Polysaccharides* **137**, 402 (2016)
28. *Electrochimica Acta* 172 (2015) 7–11.
29. L. Bao, X. Chen, B. Yang, Y. Tao, Y. Kong, *Acs Appl Mater Interfaces* **8**, 21710–21720 (2016)
30. W. Lan, H. Li, Y. Liu, *Coatings* **8**, 291 (2018)
31. T. Kawasaki, T. Nakaji-Hirabayashi, K. Masuyama, S. Fujita, H. Kitano, *Colloids Surf., B* **139**, 95–99 (2016)
32. Y. Peng, D.J. Gardner, Y. Han, Z. Cai, M.A. Tshabalala, *J. Colloid Interface Sci.* **405**, 85–95 (2013)
33. B. Kaczmarek, A. Sionkowska, J., Stojkowska, *Polym. Testing* **68**, 229–232 (2018)
34. K. Daiki, F. Tetsuya, T. Hiroshi, *Int. J. Biol. Macromol.* **126**, 54–59 (2018)
35. H. Pei, F. Chen, X. Niu, Q. Jia, R. Guo, N. Liu, Z. Mo, *J. Electroanal. Chem.* **895**, 115525 (2021)
36. R. Nurizzah, L. Darvina, A. Shahrul, A.S. Fatimah, S.L. Faridah, Y. Norazah, *Journal of electroanalytical chemistry* (2017) S1572665717304666.
37. A. Pwc, M. B, B. Hms, B. Kss, W. Kong, *Optical Materials* 114.
38. J. Qian, W. Zhonglong, L. Mingxin, S. Jie, Y. Yiqin, X. Xu, X. Haijun, W. Shifa, *Photochem. Photobiol. Sci.* **19**, 49–55 (2020)
39. A. Cz, A. Jq, L.A. Meng, B. Yy, Z. Hu, G. Yong, *J. Photochem. Photobiol. A* **40**, 429 (2021)
40. A. Fy, Z.A. Peng, B. Cd, *Microchem J* **162**, 105880 (2021)
41. P. Sun, K. Xu, S. Guang, H. Xu, *Colloids Surf., A* **609**, 125658 (2021)

Publisher's Note Springer Nature remains neutral with regard to jurisdictional claims in published maps and institutional affiliations.